Air Flow Optimization and Calibration in High-Compression-Ratio Naturally Aspirated SI Engines with Cooled-EGR

SoDuk Lee, Charles Schenk, and Joseph McDonald

US Environmental Protection Agency

Abstract

As part of the U.S. Environmental Protection Agency (U.S. EPA) "Midterm Evaluation of Light-duty Vehicle Standards for Model Years 2022-2025 [1]", the U.S. EPA is evaluating engines and assessing the effectiveness of future engine technologies for reducing CO_2 emissions. Such assessments often require significant development time and resources in order to optimize intake and exhaust cam variable valve timing (VVT), exhaust gas recirculation (EGR) flow rates, and compression ratio (CR) changes. Mazda SkyActiv-G spark-ignition (SI) engines were selected by EPA for an internal engine development program based upon their high geometric compression ratio (14:1 in Europe and Japan, 13:1 in North America) and their use of a flexible valve train configuration with electro-mechanical phasing control on the intake camshaft. A one-dimensional GT-Power engine model was calibrated and validated using detailed engine dynamometer test data [2] from 2.0L and 2.5L versions of the SkyActiv-G engine. The calibrated GTPower model and a Mathworks Model-Based Calibration (MBC) tool box are being used by EPA to explore calibration and control development of intake and exhaust cam phasing, and cooled EGR flow rates to reduce CO_2 and improve brake thermal efficiency.

This paper presents initial results of a parametric study to determine appropriate rates of cooled, external EGR (cEGR); internal (residual) EGR; and control development for a future engine technology demonstration project based upon the 2.0L, 14:1 CR version of the Mazda SkyActiv-G engine. An optimization routine was used to determine a combination of intake and exhaust cam timing, light-load internal EGR, and cEGR flow rates while satisfying the constraints of engine knock, brake torque and other functional requirements. The engine model was found to be useful for rapid engine calibration development. The modeling tools developed in this work were also used to conduct an initial evaluation of the CO_2 reduction potential of a 1-point change in geometric CR, cEGR, and application of cylinder de-activation. Upon further development, the resulting fuel flow maps can subsequently serve as inputs into EPA's ALPHA [3, 4] vehicle energy model simulations.

Introduction

As part of analyses in support of the 2017-2025 Light-duty Vehicle GHG standards, EPA contracted with Ricardo PLC to project future CO_2-reduction effectiveness for specific engine technologies. One of the most effective spark ignition engine technologies evaluated by Ricardo used a combination of sequential turbocharging, engine downsizing, engine friction reduction measures, variable valve lift and valve timing, and the use of cooled, high- and low-pressure loop EGR [5]. This particular package was referred to within the analysis as EGRB (EGR-boosted). The best BSFC of the Ricardo EGRB engine package was approximately 225 g/kW-hr, corresponding to a peak brake thermal efficiency (BTE) of approximately 37%.
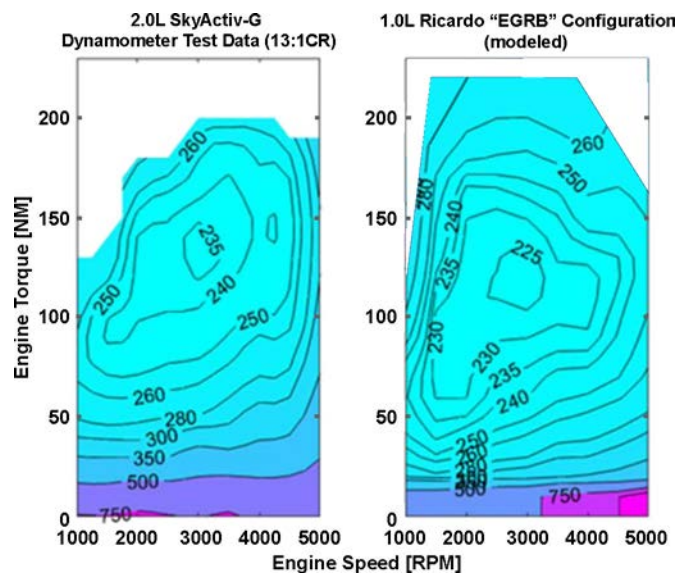

Figure 1. A comparison of BSFC maps measured for the 2.0L 13:1CR Mazda SkyActiv-G engine (left) and modeled for a 1.0L Ricardo "EGRB" configuration (right).

A recent benchmarking analysis by EPA of a 2015 Mazda SkyActiv-G naturally aspirated (NA) gasoline direct injection (GDI) engine showed a best BTE of approximately 36-37% [2], relatively

high for SI engines. This was in part due to an ability to use late-intake-valveclosing (LIVC) Atkinson-cycle operation to decouple the knock-limited effective compression ratio (CR) from the expansion ratio available from a very high 13:1 geometric CR. The Mazda SkyActiv-G is one of the first implementations of a naturally-aspirated, LIVC Atkinson-cycle engine in U.S. automotive applications outside of hybrid electric vehicles (HEV) and also appears to be the first Atkinson-cycle engine to use GDI. Port-fuelinjected (PFI) Atkinson-cycle engines have been used in hybrid electric vehicle applications in the U.S. for over a decade. PFI/Atkinson-cycle engines have demonstrated peak BTE of approximately 39% in the 2015 Honda Accord HEV and 40% in the 2016 Toyota Prius HEV [6]. While NA/Atkinson-cycle engines can achieve comparable or better peak BTE in comparison with downsized, highly boosted, turbocharged GDI engines like the Ricardo EGRB configuration, modern turbocharged GDI engines often have relatively high BTE or BSFC across a much broader range of engine speed and torque as well as improved BTE and fuel consumption at light loads, as shown in Figure 1. Based on EPA's initial engineering analysis of the Mazda SkyActiv-G engine, it appeared that another reasonable, alternative technological path to both high peak BTE and a broad range of operation with high BTE might be possible through the application of cooled-EGR (cEGR) [7], a higher geometric CR, and cylinder deactivation to a naturally-aspirated GDI/Atkinson-cycle engine like the SkyActiv-G. The goals of this work were three-fold. First, to develop an engine model using commercially available 1-D fluid dynamics and engine combustion models that could be used to conduct parametric engine technology studies and that could serve as a future basis for model-based engine calibration; second, to determine if brake thermal efficiencies comparable to GDI-turbocharged-downsized engines could be achieved by combining a naturally-aspirated, GDI, Atkinson-cycle engine with a 1-point increase in geometric CR, cooled EGR (cEGR), and cylinder deactivation (CDA); and third, to use a kinetic knock model to begin to explore whether or not moderate levels of cEGR could provide sufficient knock mitigation to allow a 1-point increase in compression ratio without changing minimum octane requirements. Mazda currently does not use cEGR in the EU-market 14:1 CR version of the SkyActiv-G, but it should be noted that Mazda requires the use of a minimum of 95-RON gasoline with this engine while the U.S. 13:1 CR version of the SkyActiv-G has a minimum 91-RON or 87 AKI requirement.

Ayala et el. presented the effects of combustion phasing, relative air-fuel ratio, compression ratio, and load on SI engine efficiency [8]. Significant increases in part-load BTE were achieved for CR above 9.8:1. An approximately 6 to 7% peak BTE improvement could be achieved at a CR of 15:1. Efficiency could also be improved with higher CR at high speeds and loads due to the reduced surface-tovolume ratio and thus reduced heat loss [8]. Lower fuel consumption and good combustion stability at part loads has also been previously achieved at high geometric CR with gasoline direct injection engines [9]. However, significantly higher BMEP and lower HC emissions were realized by using reduced geometric CR or by reducing effective CR with variable valve timing.

The use of moderate amounts of cEGR is an effective engine knock suppressant for spark ignition engines and allows advancing of combustion phasing and improving combustion stability over a wider operating range. The use of cEGR for suppressing engine knock and

its impact on peak cylinder pressure has been described by Alger et al. [7]. An approximately 50% increase in peak cylinder pressure at mid-loads was observed at 25% EGR rates when combustion phasing was advanced to Knock Limited Spark Advance (KLSA). A combination of internal and external cEGR has also been used for Controlled Auto-Ignition combustion (CAI) to reduce fuel consumption under light to part load conditions [10, 11].

Fixed CDA strategies that disable 2 or more cylinders are currently mass produced for light-duty vehicle applications. Dynamic CDA implementations that vary the relative location of deactivated cylinders are currently under development [12, 13]. Cylinder deactivation operates the remaining, firing cylinders at higher BMEP under light load conditions. This moves operation of the remaining cylinders to an area of engine operation with less throttling and thus lower pumping losses and reduced BSFC. Ford and Schaeffler investigated both dynamic and fixed CDA and found that, with appropriate vibrational dampening, either strategy could be implemented with no NVH deterioration and with 3 percent or greater improvement in both real-world and drive cycle fuel economy [13].

Methodology

An EU-market version of the 2.0L Mazda SkyActiv-G engine was selected to validate future engine technology effectiveness at a 14:1 CR and with a developmental version of low-pressure cEGR hardware. Engine calibration and control development typically requires extensive manpower and dynamometer development time. Hence, a 1-D fluid dynamics and engine combustion model using Gamma Technologies GT-Power™ engine modeling software [14] was used to accelerate the time required for hardware development and validation. Initial engine and intake airflow model development based upon the U.S. version of the 2.0L SkyActiv-G was conducted under an engineering services contract with FEV North America, Inc.

The 2.0L Mazda SkyActiv-G GDI gasoline engine was thoroughly dynamometer tested as part of a preliminary EPA benchmarking study [2]. The resulting measured engine map was converted into a GT-Power model to study the potential application of future technologies. The Mazda air box, throttle body, intake/exhaust manifold geometry, and valve lift profiles were measured to precisely model engine performance and combustion. For GT-Power engine model validation, 2.0L SkyActiv 13:1 and 14:1 compression ratio engines were tested at the EPA National Vehicle and Fuel Emissions Laboratory (NVFEL) to collect additional dynamometer test data such as intake and exhaust cam phasing, CA50, 10-90 percent burn duration, exhaust lambda (normalized air-fuel ratios), start of injection, spark ignition, and intake/exhaust pressures and temperatures.

The validated GT-Power models were then used to investigate the effects of internal EGR/external cEGR, spark timing changes, and changes to intake and exhaust cam phasing to more quickly iterate between hardware calibration and control changes than would be possible using engine dynamometer testing alone. Initial development of cEGR hardware to be used within both the model validation and subsequent engine testing was developed under an engineering services contract with Southwest Research Institute (SWRI). However, future engine calibration and controls using this hardware configuration are being developed at the EPA-NVFEL facility in Ann Arbor, Michigan. Model-based engine calibrations were analyzed

using a standard 6-core-CPU desktop computer during early stages of model development. Model-based engine calibrations will eventually be used to provide the initial test points for further enginedynamometer validation. Dynamometer tests were often used to confirm or provide additional input data as part of a feedback loop to the model-based calibration.

Model Calibration and Validation

A Three Pressure Analysis (TPA) within the GT-Power model was used to correlate in-cylinder pressure data between the engine-dynamometer-measured test data and model simulations. The crank angle based intake port and exhaust pressure data were measured by pressure transducers located adjacent to cylinder #1. Crank-angle based in-cylinder pressure traces vary somewhat from cylinder-tocylinder. Hence, the #1 cylinder pressure traces were used since they were directly related to measured intake/exhaust port pressure traces measured adjacent to cylinder #1 (Figure 2). The measured HC concentration in PPM_C3 and CO concentration in PPM were also used as inputs into the TPA model.
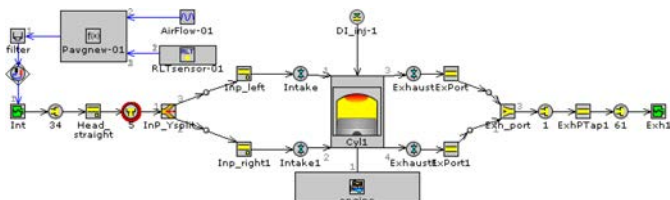
Figure 2. TPA model and pressure trace inputs.

As shown in Figure 3, the measured in-cylinder pressure traces (in blue) are in good agreement with the model estimated pressure traces (in in red). The mass-fraction-burn rates from the TPA analysis were used for correlation with the measured mass-fraction-burn rates from dynamometer testing.
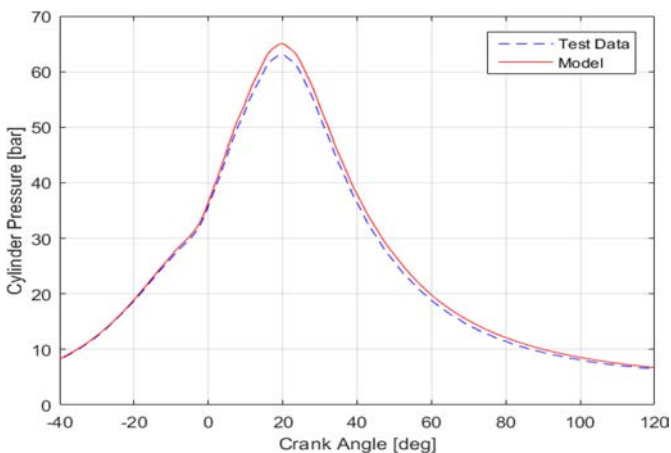

Figure 3. Crank-angle based cylinder pressure traces. Modeled values are shown in red. Measured values from engine dynamometer testing are shown in blue dotted line.

Model Validation at Full Load

Measuring the lower/upper air-box and intake plenum volumes was quite challenging since the complicated shape of the intake manifold contains significant curvature and a number of small holes (Figure 4). The intake volume was estimated by carefully filling the manifold with measured quantities of water. The air filter in the air-box was

modeled by using "OrificeConn", a standard GT-Power template with 1.9mm hole diameter and 1300 holes. The hole diameters and number of holes were tuned to minimize the differences between measured and simulated intake manifold and exhaust manifold pressures.

The throttle angle was fixed to 90 degrees for full load simulations. The simulated Intake Manifold Absolute Pressure (MAP) traces, as shown in Figure 5 (red line), were in good agreement with the measured MAP traces (blue line).

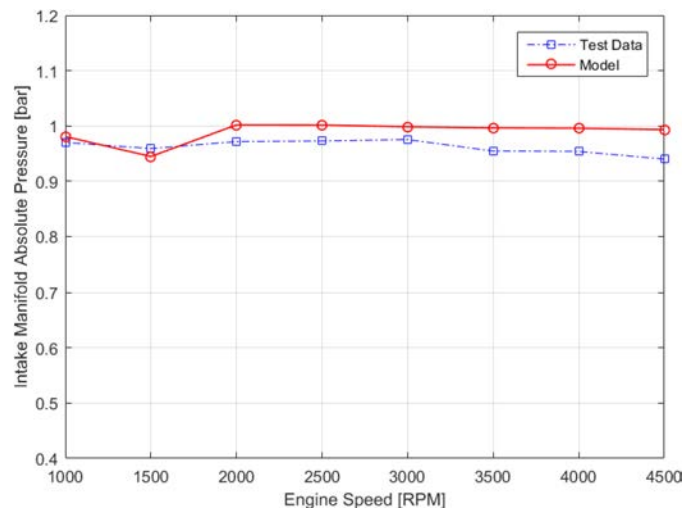Figure 4. Mazda SkyActiv engine intake manifold plenum.

Figure 5. Intake manifold absolute pressure traces. Modeled values are shown in red. Measured values from engine dynamometer testing are shown in blue dotted line with the 'O' symbol.
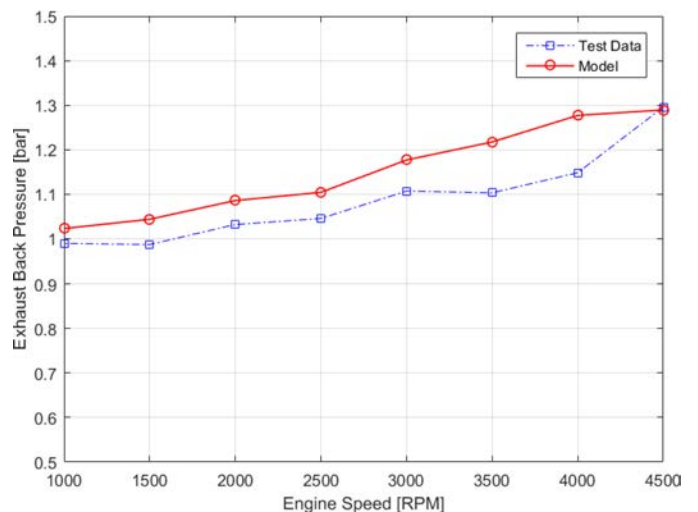

Figure 6. Modeled (red) and measured (blue) exhaust EBP traces.

As shown in Figure 6, the simulated exhaust back pressure (EBP) traces (red line) were also in good agreement with the measured exhaust pressure traces (blue line).
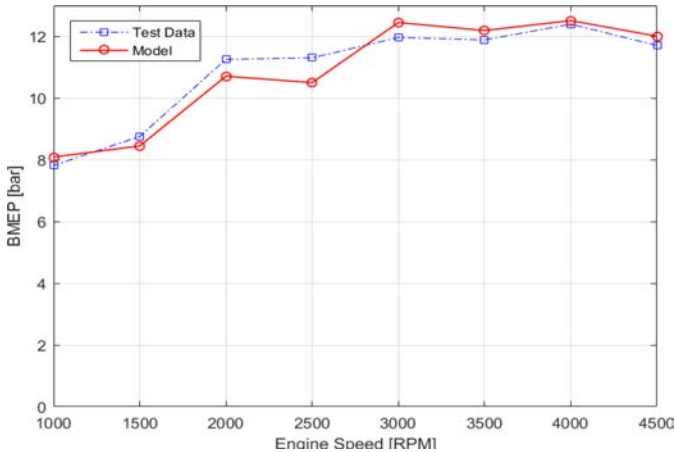

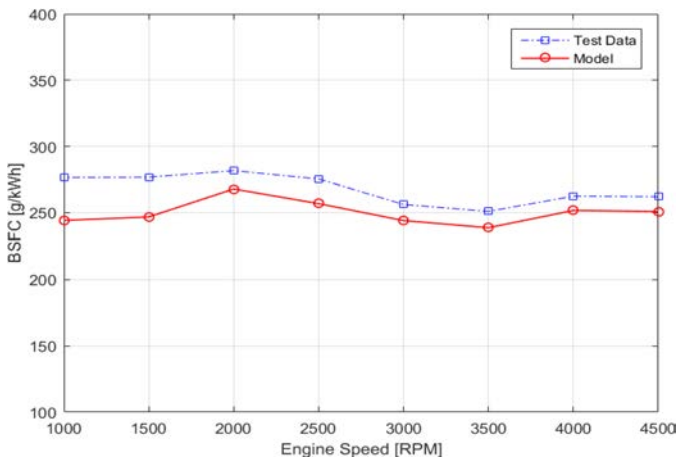Figure 7. Modeled (red) and measured (blue) BMEP at full load.

Figure 8. Modeled (red) and measured (blue) full load BSFC

Figure 7 shows that the simulated full load engine BMEP traces were in good agreement with the measured BMEP traces. The model was able to simulate the manifold wave dynamics and tuning effects and approximately matched the shape of the plot of full load engine torque vs. engine speed throughout the entire engine speed range. At 3250 RPM/WOT, the volumetric efficiency of the 2.0 L naturally aspirated SkyActiv-G engine was slightly greater than 100% due to its well-designed intake and exhaust manifold. The full load engine torque at 2500 RPM engine speed was also somewhat less than that at 1750 and 2000 RPM engine speeds. After final tuning of the modeling parameters, the simulated engine torque traces exactly followed the measured engine torque traces from 1750 to 4000 RPM engine speeds The measured and simulated Brake Specific Fuel Consumption (BSFC) were generally in agreement (Figure 8). The differences between test data and model ranged from 1% to 5%, and average differences were approximately 3%.

Model Validation at Part Load

The throttle angles in the standard GT-Power "throttle object" were automatically adjusted using a modeled throttle control routine during the part load simulations. Figure 9 shows that the modeled manifold

pressure (red) was in good agreement with the measured values (blue). As shown in Figure 10, the measured exhaust back pressure traces shown with the blue colored line were slightly higher, but the pressure trends between the measured and the simulated exhaust pressure traces were in good agreement.
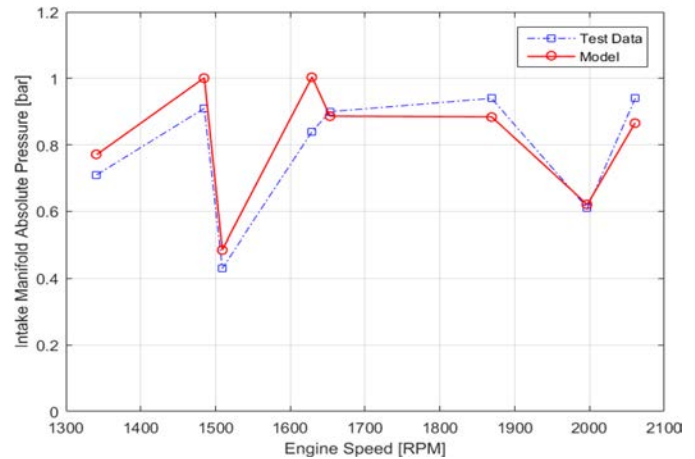

Figure 9. Modeled (red) and measured (blue) intake manifold absolute pressure traces at part-load.
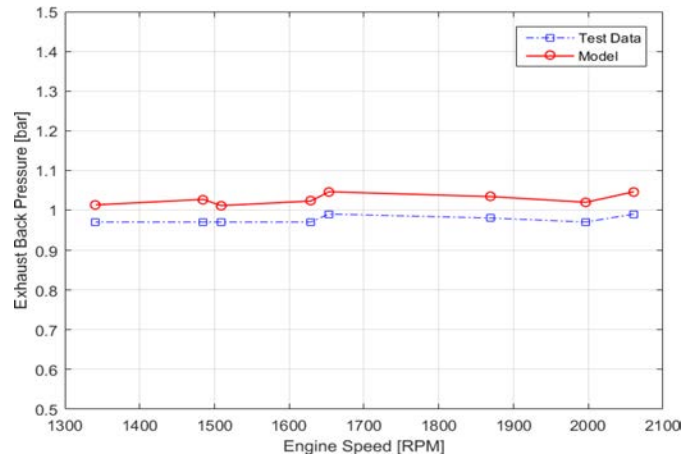

Figure 10. Modeled (red) and measured (blue) EBP pressure traces at part-load.
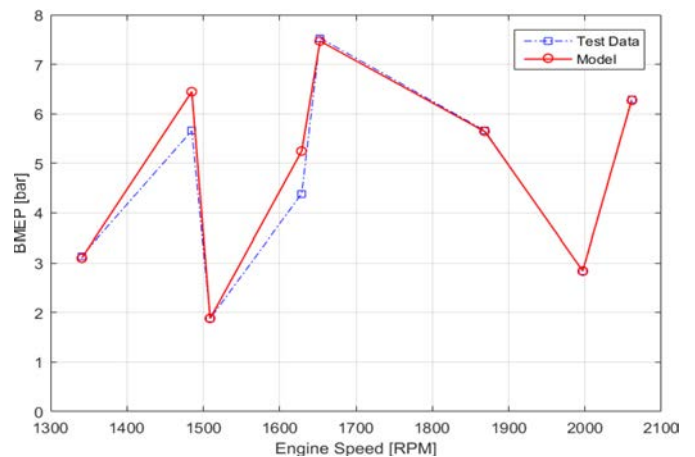

Figure 11. Modeled (red) and measured (blue) part-load engine BMEP.

The measured and the simulated engine brake torque, as shown in Figure 11, were also in good agreement at part loads.

As shown in Figure 12, brake specific fuel consumption (BSFC) from the model simulations was somewhat higher than measured values from dynamometer testing although the simulated and the measured BSFC curves are in good agreement. This may be caused by small errors in the look-up table based Friction Mean Effective Pressure (FMEP) values used during modeling. A factor of about 0.006 of peak cylinder pressure was used to estimate firing FMEP based upon the lookup table values for motoring FMEP. Small FMEP differences result in more noticeable BSFC differences at part loads. However, the measured and the simulated BSFC are in good agreement in general. Additional work to carefully determine motored FMEP for this engine is expected to more closely match modeled FMEP to actual FMEP and should improve BSFC correlation between modeled and measured results as model development for this engine continues.
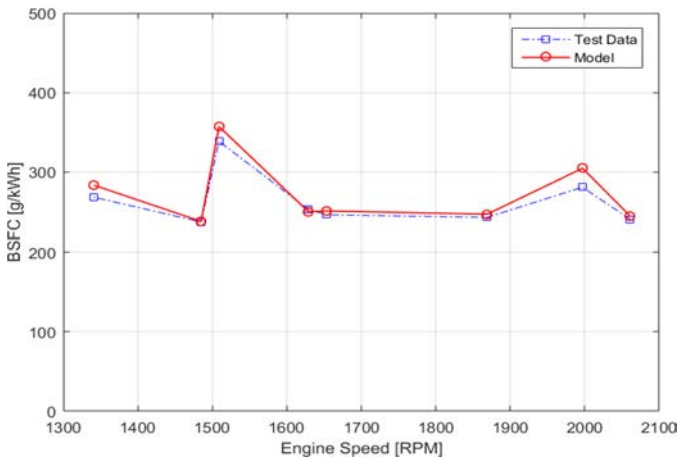

Figure 12. Modeled (red) and measured (blue) part-load BSFC.

Engine Technology "Futuring" and Model Applications

The purpose of engine "futuring" within regulatory analyses is to estimate the efficiency of engines and engine technologies that may be applied in the 2022~2025 MY timeframe. Engine "futuring" is typically performed by EPA starting with base engine maps measured through our own internal benchmarking methodologies. As a quality control check, the final engine maps are often reviewed by vehicle manufacturers, component suppliers and/or are compared with publicly available data (if available) to verify accuracy. Engine technologies can then be applied to these engines using GT-Power to model the effectiveness of each of the individual technologies. In this manner, additional engine performance metrics, such as knock mitigation, can also be assessed.

Following initial model validation, the GT-Power model of the Mazda SkyActiv-G engine was used to investigate the effects of a higher compression ratio, CDA, cEGR, and valve timing changes. Technology effectiveness of these potential future engine configurations was estimated by comparing relative BSFC (Brake Specific Fuel Consumption) improvements relative to the 2.0L SkyActiv-G base 13:1 CR U.S. version of the engine. A kinetic knock model was also used to compare knock-limited engine operation between potential future configurations and the base engine configuration. A measured lower heating value (LHV) of 42.9 MJ/kg for the 96 RON Tier 2 certification gasoline used during engine testing was also used to calculate Brake Thermal Efficiency (BTE) from modeled and actual BSFC. Dynamometer test data were

collected at more than 200 engine speed and torque conditions. The 2.0L SkyActiv-G compression ratio 13:1 base engine maps as shown in Figure 13 were created from steady state engine dynamometer test data. As shown in Figure 14, the BSFC map from GT-Power modeling is in good agreement with the BSFC map generated from dynamometer test data. Model estimated BSFC was higher below 0.5 bar BMEP load and GT-Power sometimes estimated unreasonably high BSFC at 0 bar BMEP load. The simulated target BMEPs were from 0.5 bars to 13 bars. Hence, BSFC values at the below 0.5 bar BMEP were estimated by using a low fidelity extrapolation method.
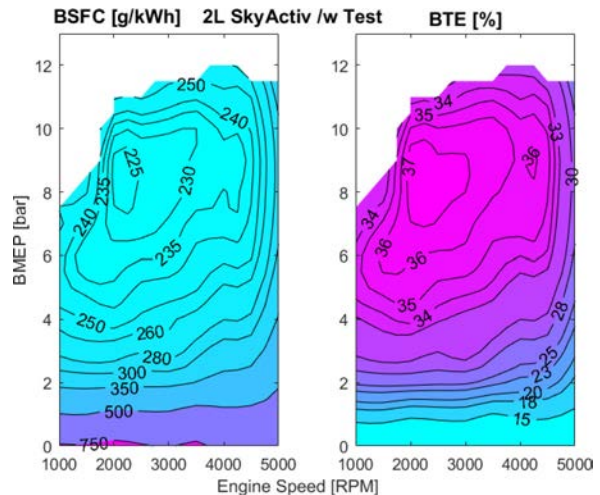

Figure 13. Base 2.0L Mazda SkyActiv 13:1 CR engine maps of BSFC (left) and BTE (right) from dynamometer test data.
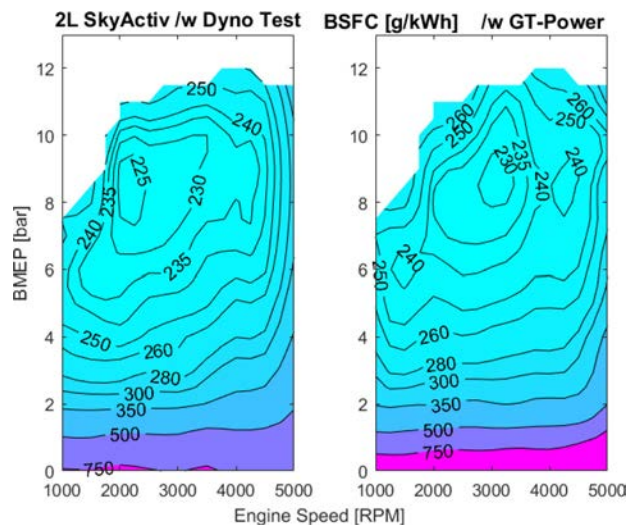

Figure 14. Comparison of measured (left) and modeled (right) BSFC for the 2.0L SkyActiv-G at 13:1 CR.

Compression Ratio (CR) Effectiveness

The modeled BSFC change of increasing geometric CR from 13:1 to 14:1 is shown in Figure 15. This BSFC map at 14:1 CR could not be validated with engine dynamometer operation, even with use of 96 RON E0 fuel, due to the onset of knock. The likelihood of knock occurring with the 14:1 CR engine was further investigated by modeling the Knock Induction Time (KIT) Integral values generated using GT-Power at 13:1 CR and at 14:1 CR both without and with cEGR.
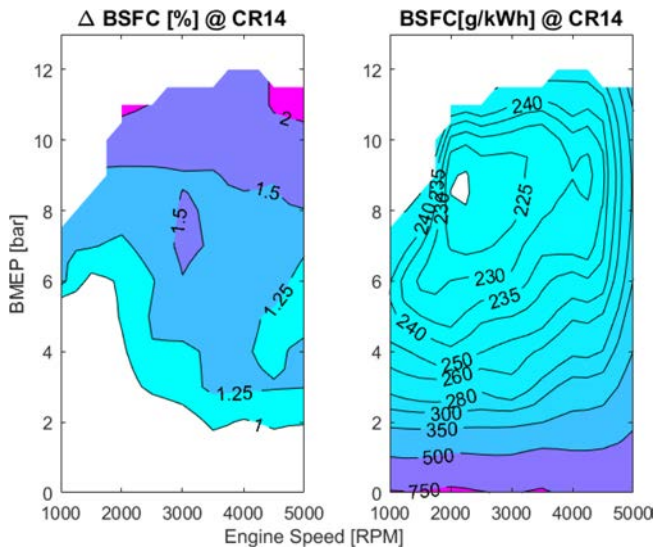
Figure 15. The percentage improvement in BSFC (left) for increasing CR from 13:1 to 14:1 and the resulting BSFC map for 14:1 CR (right).

In the 'kinetic-fit' knock model used within the GT-Power engine model, the following equation is used to compute three induction times for low, intermediate and high temperature regions:

$$\tau_i = M_1 a_i \left(\frac{ON}{100}\right)^{b_i} [Fuel]^{c_i} [O_2]^{d_i} [Diluent]^{e_i} Exp\left(\frac{f_i}{M_2 T}\right) \quad i = 1, 2, and\ 3,$$

where τ_i is the induction time at the instantaneous temperature and pressure for the mixture in region i, M_1 is the Knock Induction Time Multiplier, ON is the Fuel Research Octane Number, M_2 is the Activation Energy Multiplier, $[Fuel]$, $[O_2]$, and $[Diluent]$ are concentrations expressed in mol/m^3, and a_i through f_i are model constants. $Diluent$ concentration is the sum of concentrations of N_2, CO_2, and H_2O. The knock threshold at induction time τ is assumed to be reached under the following conditions:

$$\int_{t_0}^{t_i} \frac{dt}{\tau} = 1$$

where t is the elapsed time from the start of the end-gas compression process and t_i is the time of auto-ignition.

Gas temperatures increase with increasing compression ratio and therefore the likelihood of knock is increased for the decreased induction times that occur at higher compression ratios. The modeled KIT increased as compression ratio increased from 13:1 to 14:1 and an increased potential for knock onset appears likely at the higher compression ratio even with 96 RON fuel. However, as shown in Figure 16, adding low-pressure cooled EGR decreased the KIT to approximately the same levels or somewhat improved levels compared with the base 13:1 CR engine when modeled using either 96 RON or 91 RON gasoline. There was also a moderate impact on KIT at higher speed and load conditions that may be due in part to subtle changes in intake manifold geometry from implementation of the EGR system hardware and in part to re-optimized spark timing.

The KIT results indicate that a 14:1 CR engine with cEGR is likely to be at least as knock tolerant as the original U.S. 13:1 CR version of the Mazda SkyActiv-G engine. Further engine testing is underway at EPA-NVFEL to validate the GT-Power kinetic knock modeling results for these engine configurations.
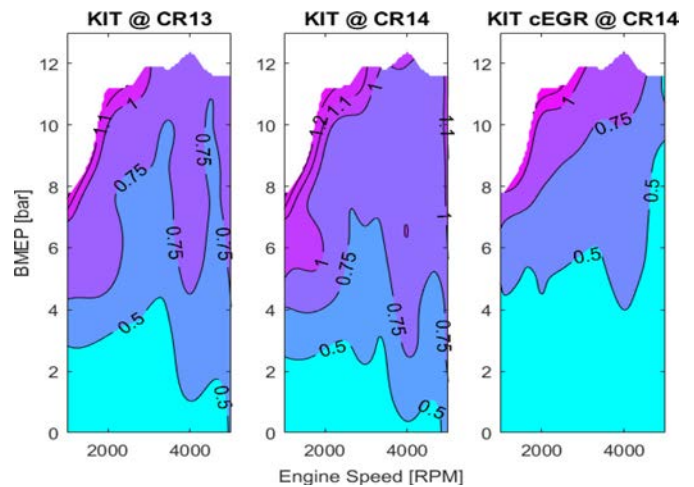
96 RON E0.
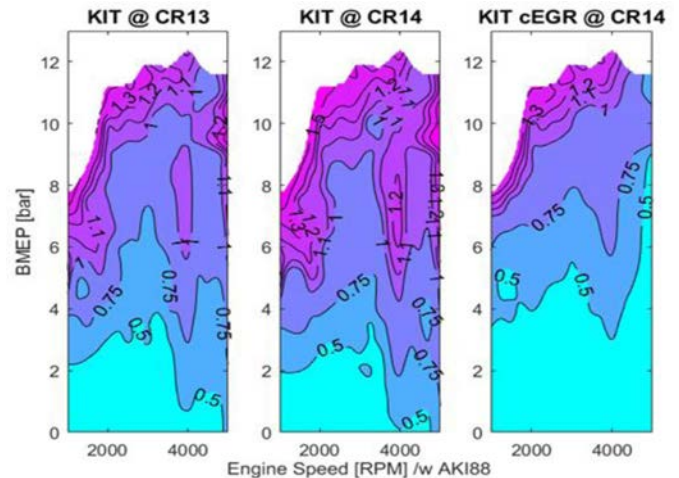
91 RON E10.

Figure 16. Modeled KIT is shown for three different engine configurations (left, 13:1 CR; middle, 14:1 CR; right, 14:1 CR and Cegr) and two different fuels (top, 96 RON E0 Tier 2 certification gasoline; bottom, 91 RON E10 LEV III certification gasoline).

Cylinder De-Activation (CDA) Effectiveness

As shown in Figure 17, the 2.0L Mazda SkyActiv-G engine model was modified to simulate de-activation of 2 cylinders below 3000 rpm and 5 bar BMEP load. The fuel injector object within the model had to be modeled as individual injectors since deactivated cylinders are modeled with different air-fuel ratio than the active cylinders. The air-fuel ratios in the deactivated cylinders are infinite while nearstoichiometric air fuel ratios are maintained in the active cylinders. Intake and exhaust valve lifts were set to zero. No spark ignition was used in the deactivated cylinders. A larger reduction in BSFC was achieved by reducing pumping losses via use of larger intake throttle openings. Achieving the target BMEP with 2 cylinder deactivation was not possible by using the original intake valve cam

phasing. The active intake valves had to be opened earlier to achieve the desired air flow and BMEP levels. The CDA effects as shown in Figure 18 were different depending on engine speeds and loads.
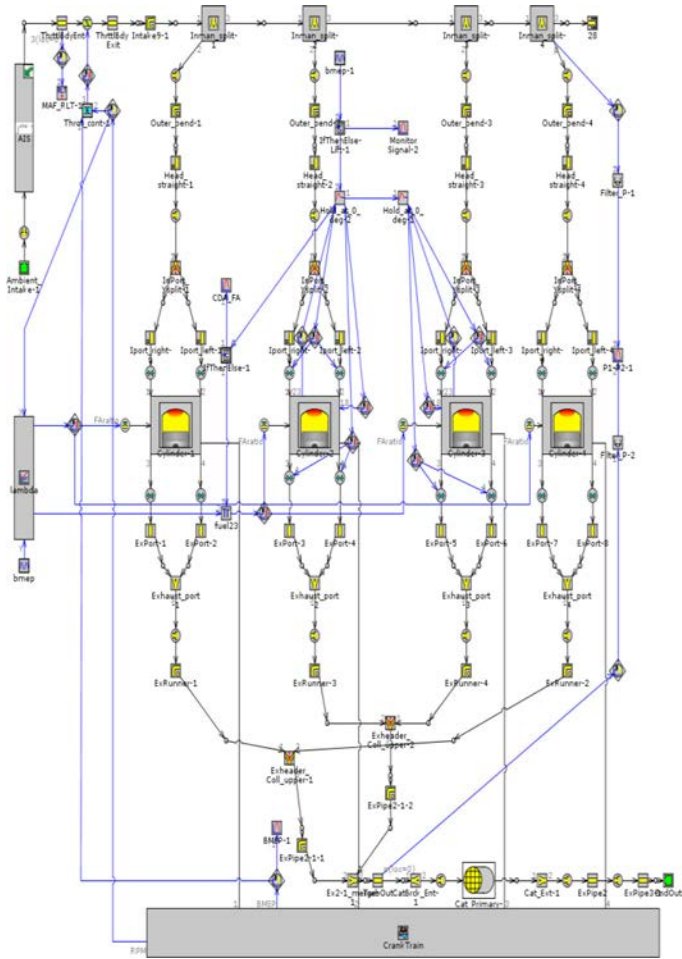

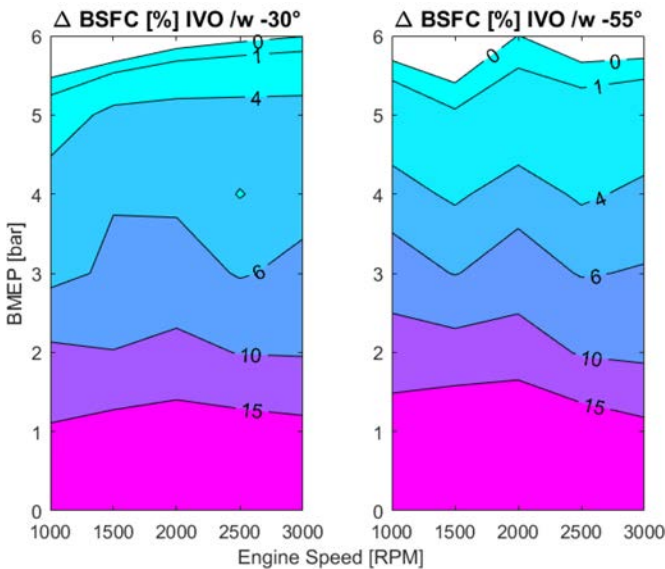Figure 17. A CDA version of the GT-Power 4 cylinder model.

Figure 18. Combined impacts of CDA and two different intake valve opening timings.

The GT-Power optimizer was useful to automatically optimize IVO timing while attempting to maximize CDA effectiveness. The CDA effectiveness from the SkyActiv-G model simulation was comparable

to that achieved during dynamometer testing of a GM Chevrolet Silverado equipped with cylinder deactivation [15] (Figure 19). Two cylinders were de-activated during testing of the 4.3L, 6 cylinder GM engine. The simulated CDA effectiveness obtained in the SkyActiv-G modeling was somewhat higher, which may in part be due to the modeled 50% CDA (4 cylinders to 2 cylinders) relative to the 33% CDA measured in the GM application (6 cylinder to 4 cylinder). It should be noted that further research will be necessary to determine the frequency that CDA can be employed over the regulatory drive cycles and during in-use driving.
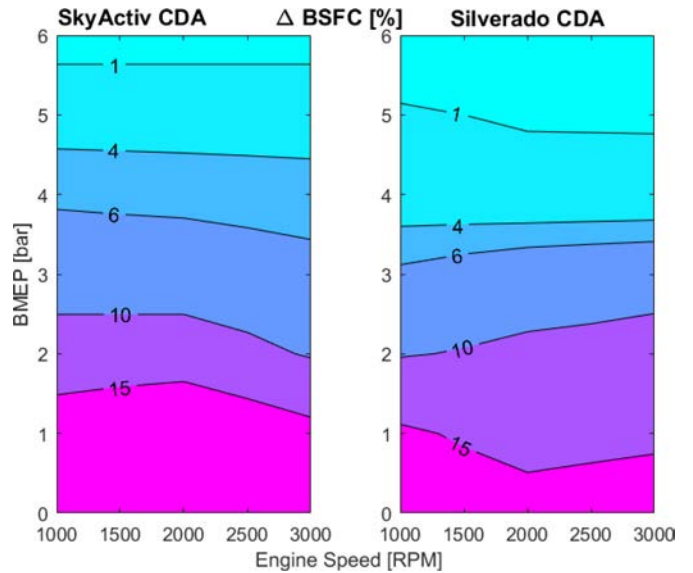

Figure 19. Comparison of CDA effectiveness modeled for the "futured" SkyActiv-G and measured for the GM 4.3L V6.
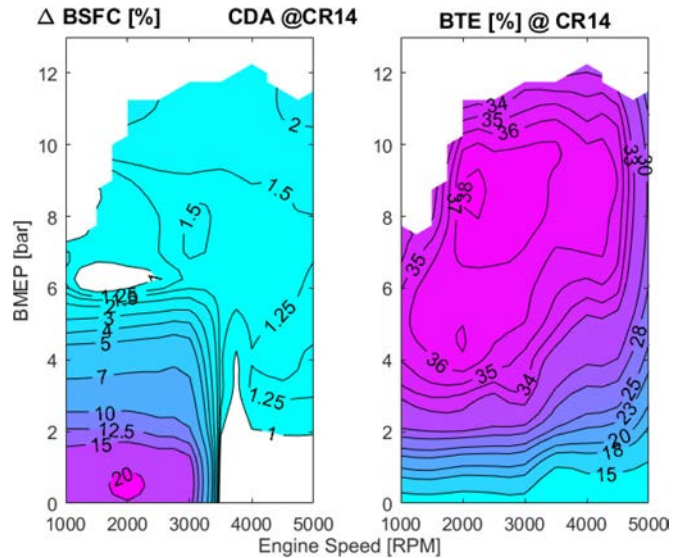

Figure 20. The combined impact of CDA and CR changes. The percentage improvement in BSFC shown on the left and the resulting BSFC map is shown on the right.

CDA can impact noise, vibration and harshness (NVH) and may impact blowby and engine durability. EPA's benchmarking of the Silverado 4.3L engine w/CDA showed that although the engine may be capable of running in deactivation mode in the speed and BMEP range modeled for this engine, there may be NVH, emissions control, or other reasons to restrict CDA operation to meet overall vehicle requirements. The Silverado 4.3L engine, for example, used CDA for

roughly half of the time within its CDA-capable range over the FTP75 and HwFET regulatory drive cycles. NVH countermeasures can be used to expand the operational range of CDA. Recent work by Schamel et al. demonstrated the effectiveness of a dual mass flywheel (DMF) and circumferential pendulum absorber for further addressing CDA NVH issues [13]. Alternating and/or dynamically changing the cylinders that are deactivated may also increase the range of operation for implementing CDA [12, 13, 16]. When modeling CDA together with a 1-point increase in CR on the SkyActiv-G, the estimated 35% BTE envelope (as shown in Figure 20) was increased below 6 bar BMEP load, and at engine speeds from 1000 to 3000 RPM compared to the base 13:1 BTE map in the Figure 13. Combining CR and CDA without cEGR may not be a viable combination due to elevated modeled KIT values and thus potential for knock onset.

Cooled EGR (cEGR) Effectiveness

The low pressure, cEGR system was developed using an EGR throttle body, EGR valve, mixer, and EGR cooler. The EGR valve body is connected between the air box and the EGR mixer. The EGR cooler is located between the EGR valve body and the catalyst entry connecting pipe. The EGR target values initially developed by SWRI are shown in the left of Figure 21 and were implemented as a lookuptable in the GT-Power model. The EGR controller automatically adjusted to the proper EGR rates as shown in the right side of Figure 21 depending on speed-load points. The EGR throttle body is used to create vacuum pressure to induce the EGR flow from near the entrance to engine's exhaust catalyst. As shown in Figure 22, increased BSFC benefits were realized at part-loads with cEGR [17, 18]. Further optimization of EGR rates is possible and is planned for subsequent modeling and engine dynamometer testing. As shown in Figure 22, a 2~5% improvement in BSFC was achieved with cEGR effectiveness when excluding compression ratio effects. This is comparable to previously demonstrated results [19]. The relative effectiveness and BSFC for the combined effects of 14:1 CR and cEGR are shown in Figure 22.
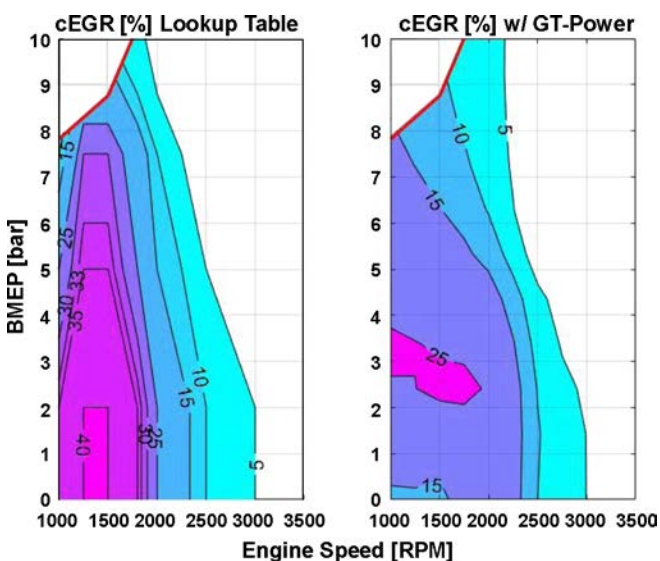

Figure 21. Rates of cEGR targeted as part of the SWRI system design (left) compared with modeled cEGR rates (right).
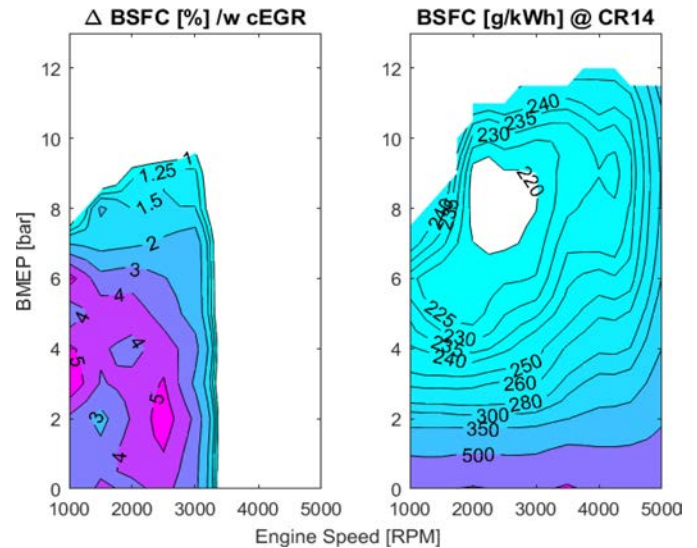

Figure 22. The percentage improvement in BSFC due to cEGR is shown on the left. A BSFC map with the combined impact of cEGR and a 14:1 CR is shown on the right.

CR + Cooled EGR (cEGR) + CDA Effectiveness

The BSFC and BTE maps in Figures 23 and 24 were generated by using a combination of 14:1 CR, cEGR and CDA GT-Power modeling results. The resulting BSFC map (Figure 25, left side) approaches the effectiveness of the 2020MY Ricardo EGR boosted (EGRB) engine map (Figure 25, right side) over most of the range of engine speed vs. torque with the exception of operation at very low speeds (<1500 rpm) and light loads (< 40 N-m).
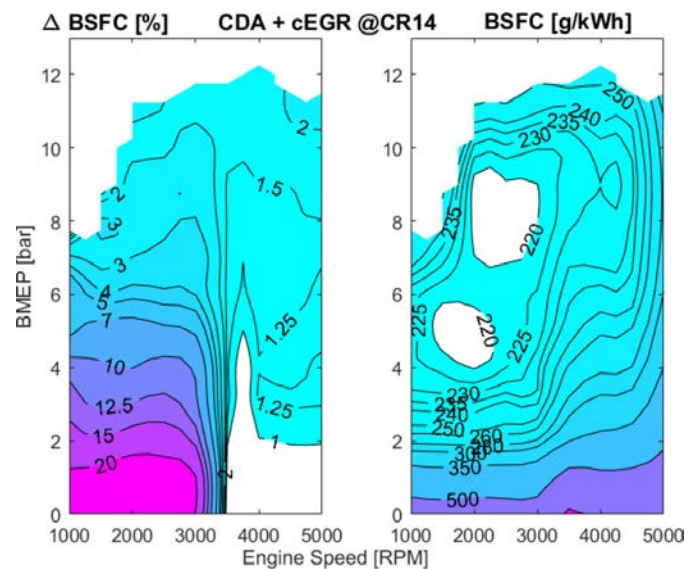

Figure 23. The combined impact of cEGR, a 1-point increase in CR and CDA (entire "futured" configuration). The percentage improvement in BSFC is shown on the left and the resulting BSFC map is shown on the right.
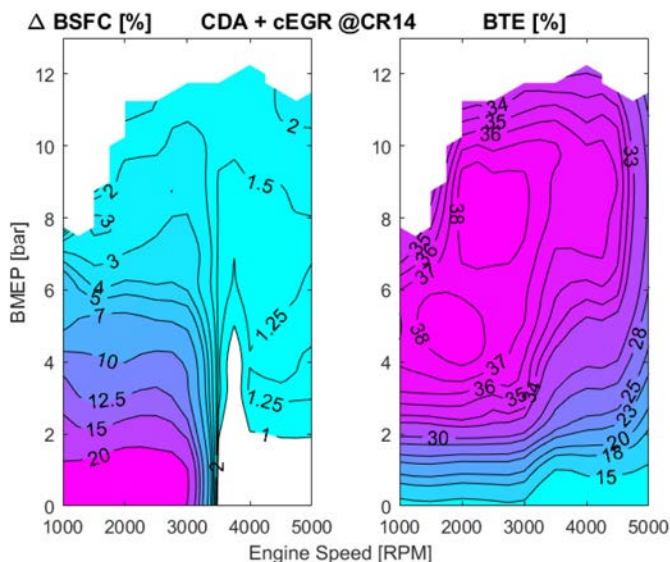
Figure 24. The combined impact of cEGR, a 1-point increase in CR and CDA (entire "futured" configuration). The percentage improvement in BTE is shown on the left and the resulting BTE map is shown on the right.
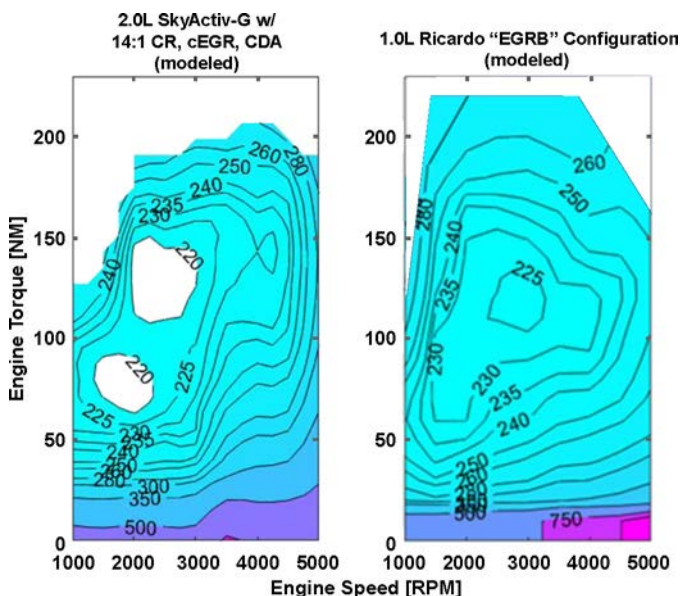

Figure 25. A comparison of BSFC maps modeled for the "futured" 2.0L SkyActiv-G engine (14:1 C.R., cEGR, CDA, left) and modeled for a 1.0L Ricardo "EGRB configuration"(right).

Summary/Conclusions

2.0L and 2.5L Mazda SkyActiv-G engines were tested at the dynamometer test facility at EPA Ann Arbor NVFEL laboratory. A 2.0L Mazda SkyActiv-G engine was chosen to demonstrate future engine technology effectiveness. The 14:1 CR version of the engine with the low-pressure cEGR hardware is currently under development at NVFEL. A GT-Power engine model was used to study and accelerate engine hardware calibration and control development. The model was found to be quite useful to understand and investigate the combined synergies and the potential effectiveness of various engine technologies. The modeled configuration of 14:1 CR, cEGR and CDA showed significant promise as a means to expand the area of the speed/load range of the engine at above 35-37% BTE.

Engine map generation was a by-product of this ongoing study and allowed an initial analysis of engine "futuring" approaches. The resulting engine map developed during modeling can be used to provide input into future EPA ALPHA vehicle modeling to estimate CO2 drive cycle effectiveness over the FTP, HwFET and other regulatory drive cycles and at different vehicle road-loads.

A transparent process has been developed and validated at EPANVFEL to quickly estimate the effectiveness of various future engine technologies such as variable valve timing (VVT), CDA, cEGR and other technology and calibration effects. A kinetic knock model and Knock Induction Time (KIT) integral simulations were also used to analyze the use of a cEGR implementation for mitigating engine knock for a geometric CR increase from 13:1 to 14:1 while further increasing engine efficiency. The KIT simulations suggest that a 14:1 CR version of the SkyActiv-G engine with cEGR likely has knock tolerance comparable to the 13:1 CR U.S. market SkyActiv-G engine.

Future Work

The GT-Power model simulation results such as cEGR flow rates, EGR valve angles, spark ignition, and cam phasing will be used to determine offset values within the existing engine calibration or as initial starting points for new calibrations. A "futured" SkyActiv-G engine with cEGR and CDA appears to be a promising alternative engineering path without the use of turbocharging and will be the subject of further EPA engine modeling and engine dynamometer research in support of the Light-duty Vehicle Midterm Evaluation. The low pressure/cEGR and 14:1 compression ratio engine hardware are currently undergoing dynamometer testing at EPA-NVFEL, and GT-Power and model-based calibration methodology will be heavily employed to accelerate advanced engine technology implementation and further calibration development.

References

1. U.S. Environmental Protection Agency and Department of Transportation, "2017 and Later Model Year Light-duty Vehicle Greenhouse Gas Emissions and Corporate Average Fuel Economy Standards: Final Rule, "Federal Register vol. 77, no 199, October 15, 2012.

2. Ellies, B., Schenk, C., and Dekraker, P., "Benchmarking and Hardware-in-the-Loop Operation of a 2014 MAZDA SkyActiv 2.0L 13:1 Compression Ratio Engine," SAE Technical Paper 2016-01-1007, 2016, doi:10.4271/2016-01-1007.

3. Lee, B., Lee, S., Cherry, J., Neam, A. et al., "Development of Advanced Light-Duty Powertrain and Hybrid Analysis Tool," SAE Technical Paper 2013-01-0808, 2013, doi:10.4271/2013-01-0808.

4. Lee S., PhD, Lee, B., Zhang H., PhD, Sze C. PhD, et al., "Development of Greenhouse Gas Emissions Model for 2014-2017 Heavy- and Medium-Duty Vehicle Compliance," SAE Technical Paper 2011-01-2188, 2011, doi:10.4271/2011-01-2188.

5. Ricardo, "Computer Simulation of Light-Duty Vehicle Technologies for Greenhouse Gas Emission Reduction in the 2020-2025 Timeframe," EPA-420-R-11-020, 2011

6. Takahashi, D., Nakata, K., Yoshihara, Y., Ohta, Y. et al., "Combustion Development to Achieve Engine Thermal Efficiency of 40% for Hybrid Vehicles," SAE Technical Paper 2015-01-1254, 2015, doi:10.4271/2015-01-1254.

7. Alger, T., Gukelberger, R., Gingrich, J., and Mangold, B., "The Impact of Cooled EGR on Peak Cylinder Pressure in a Turbocharged, Spark Ignited Engine," *SAE Int. J. Engines* 8(2):455-463, 2015, doi:10.4271/2015-01-0744.

8. Ayala, F., Gerty, M., and Heywood, J., "Effects of Combustion Phasing, Relative Air-fuel Ratio, Compression Ratio, and Load on SI Engine Efficiency," SAE Technical Paper 2006-01-0229, 2006, doi:10.4271/2006-01-0229.

9. Kramer, F., Schwarz, C., and Witt, A., "Effect of Compression Ratio on the Combustion of a Pressure Charged Gasoline Direct Injection Engine," SAE Technical Paper 2000-01-0250, 2000, doi:10.4271/2000-01-0250.

10. Cairns, A., Blaxill, H., and Irlam, G., "Exhaust Gas Recirculation for Improved Part and Full Load Fuel Economy in a Turbocharged Gasoline Engine," SAE Technical Paper 2006-01-0047, 2006, doi:10.4271/2006-01-0047.

11. Bauer, M., "Cooled EGR shows benefits for gasoline engines," Automotive Engineering Article, September 2014

12. Wilcutts, M., Switkes, J., Shost, M., and Tripathi, A., "Design and Benefits of Dynamic Skip Fire Strategies for Cylinder Deactivated Engines," *SAE Int. J. Engines* 6(1):278-288, 2013, doi:10.4271/2013-01-0359.

13. Schamel, A., Scheidt, M., Weber, C. Faust, H. "Is Cylinder Deactivation a Viable Option for a Downsized 3-Cylinder Engine?" Vienna Motor Symposium, 2015.

14. Zhong, L., Musial, M., Resh, W., and Singh, K., "Application of Modeling Technology in a Turbocharged SI Engine," SAE Technical Paper 2013-01-1621, 2013, doi:10.4271/2013-01-1621.

15. Stuhldreher, M., "Fuel Efficiency Mapping of a 2014 6-Cylinder GM EcoTec 4.3L Engine with Cylinder Deactivation," SAE Technical Paper 2016-01-0662, 2016, doi:10.4271/2016-01-0662.

16. Cecur, M., Tomiska, L. "Cylinder deactivation for CO2 reduction of 3-cylinder gasoline engines," International Engine Congress, Baden Baden Germany, February 18-19, 2014.

17. Siokos, K., Koli, R., Prucka, R., Schwanke, J. et al., "Assessment of Cooled Low Pressure EGR in a Turbocharged Direct Injection Gasoline Engine," *SAE Int. J. Engines* 8(4):1535-1543, 2015, doi:10.4271/2015-01-1253.

18. Hoepke, B., Jannsen, S., Kasseris, E., and Cheng, W., "EGR Effects on Boosted SI Engine Operation and Knock Integral Correlation," *SAE Int. J. Engines* 5(2):547-559, 2012, doi:10.4271/2012-01-0707.

19. Shutty J. and Czarnowski R., "Control strategy for a dual loop EGR system to meet Euro 6 and Beyond,", 2009 DEER conference, 2009, Dearborn, Michigan.

Contact Information

SoDuk Lee, Ph.D.
Assessment & Standards Division
US EPA - Office of Transportation & Air Quality
2000 Traverwood Drive, Ann Arbor, MI 48105
734-214-4373
lee.soduk@epa.gov

Acknowledgments